

## ACOUSTIC-SURFACE-WAVE RESONATORS FOR BAND-PASS FILTER APPLICATIONS\*

By

G. L. Mattheai, F. Barman, and E. B. Savage  
University of California  
Electrical Engineering and Computer Science  
Santa Barbara, California 93106

### Abstract

Acoustic-surface wave resonators provide a possibility for obtaining very small, high-Q resonators for frequencies up into the low microwave range. A surface-wave resonator consists of two arrays of reflectors with one or two interdigital transducers in between, fabricated on the surface of a piezoelectric substrate. The two transducer form of these resonators is particularly attractive for band-pass filter applications.

### Introduction

Bulk-wave crystal resonators have long provided a means for obtaining small, high-Q ( $Q = 10,000$  to  $300,000$ ) resonators in the frequency range from kHz to about 50 MHz for fundamental operation. At higher frequencies the crystal plate becomes too small to be practical. Acoustic-surface-wave resonators provide a means for getting around the frequency limitations of bulk-wave crystal resonators. The surface-wave resonator structure consists of arrays of metal or other reflecting elements fabricated on the crystal surface by methods similar to those used in integrated circuits. Such resonators may be useful for applications up to the lower microwave range since it is possible to fabricate very small structures on a surface.  $Q$ 's of surface-wave resonators are generally not as high as their bulk-wave counterparts, but example designs to date have exhibited unloaded  $Q$ 's of the order of 1500 up to tens of thousands, depending upon the particular substrate material and design. A sizeable amount of recent work on surface-wave resonators is reported in references 1 and 2.

### One-Port Surface-Wave Resonators

Figure 1(a) shows a one-port version of the type of resonator under consideration. To the left and the right are arrays of reflecting elements on the surface of a piezoelectric substrate such as lithium niobate or quartz. The reflecting elements can be made of metal (typically aluminum) or can be etched grooves, or ion implantations into the substrate.<sup>1,2</sup> Each reflector element creates only a small reflection so that it is only by virtue of the cumulative effect of a large number of elements (typically 150 to 300) that a resonator property is achieved between the two arrays. In the center of the structure is an interdigital transducer with electrical connections at the small tabs above the letter A. Under the condition of resonance the interdigital transducer observes very large mechanical standing waves which by way of the piezoelectric effect are translated into an electrical resonance at the transducer terminals.

The electrical properties of the transducer in Fig. 1(a) can be modeled by quite accurate transmission-line equivalent circuits.<sup>3</sup> However, the main properties of the circuit can be modeled more simply by the equivalent circuit shown in Fig. 2 which has a reactance characteristic similar to that sketched by the solid lines on the right. The resonance at  $f_1$  in Fig. 2 is due to the elements  $L_s$  and  $C_s$  which

result from the mechanical resonance between the arrays as coupled through the interdigital transducer. The parallel capacitance  $C_o$  in Fig. 2 is the interelectrode capacitance of the interdigital transducer. Along with  $L_s$  and  $C_s$ ,  $C_o$  causes a parallel-type resonance at frequency  $f_2$ . The resistor  $R_s$  is due to mechanical losses, while the resistor  $R_f$  is caused by resistance in the fingers of the interdigital transducer. Except for  $R_f$ , the equivalent circuit in Fig. 2 is identical to the equivalent circuit for a bulk-wave crystal resonator.

As can be seen using a transmission-line model, the fractional stop-band width for the arrays will only be about 1%.<sup>3</sup> Thus it is seen that the resonator effect will necessarily be confined to a very narrow bandwidth. In a typical surface-wave resonator on lithium niobate, the frequency,  $f_2$ , indicated in Fig. 2 is only 0.1 to 0.2% above  $f_1$ . This antiresonance close to the series resonance may interfere with the desired filter pass band in some applications, and it also results in relatively small reactance at frequencies away from  $f_1$  and  $f_2$ . In Fig. 2 the dashed curve suggests the reactance of a conventional series LC circuit which has the same reactance slope at  $f_1$  as does the surface-wave resonator. Note that away from resonance the reactance of the surface-wave resonator at, say, M and P is relatively small. Thus, though both resonators will give essentially the same 3-dB bandwidth in a given circuit, the surface-wave resonator would give much less attenuation away from resonance.

One way of getting around these difficulties is to use lumped elements in conjunction with the acoustic-wave resonator.<sup>5,6,7</sup> While another is to use the resonators in lattice networks.<sup>5,6,8</sup> Still another is the use of two-port resonators discussed in the next section.

### Two-Port Resonators

Figure 1(b) shows a surface-wave resonator having two reflecting arrays with two interdigital transducers in between thus giving an electrical port at A and at B. It can be shown that the two-port resonator in Figs. 1(b) or 3(a) can be modeled approximately by the lumped-element circuit shown in Fig. 3(b) for frequencies within the stop band of the reflecting arrays.<sup>4</sup> Here  $L_n$  and  $C_n$  account for the mechanical resonance, and  $R_n$  represents mechanical loss. The

\* This research was supported by the National Science Foundation Grant Number ENG72-04059 A03.

resistances  $R_{fA}$  and  $R_{fB}$  are the resistances due to loss in the fingers of transducers A and B while the shunt capacitances  $C_A$  and  $C_B$  are the interelectrode capacitances of the two transducers. The circuit in Fig 3(b) may be further simplified as shown in Fig. 3(c). There  $L_n$ ,  $C_n$ , and  $R_n$  are the same as in Fig. 3(b). The remaining elements are slowly varying functions of frequency, but they may be regarded as constant within the bandwidth of the resonance. Note that the equivalent circuit in Fig. 3(c) shows that the two-port type of resonator will have a single resonance, and the problems associated with the one-port resonator characteristic in Fig. 2 are avoided.

The equivalent circuits in Fig. 3(b), (c) are valid within the stopband of the reflecting arrays. For frequencies outside of the stopband of the arrays there can be no surface-wave resonator effect, and the device functions much the same as a delay line having two interdigital transducers. For these frequencies the loss will be the 6-dB bidirectional loss of the transducers plus the mismatch loss between each transducer and its adjacent load.

The dashed lines and crosses in Fig. 4 show measured results for a two-port resonator on lithium niobate using 300 open-circuited, 5000Å-thick aluminum reflectors 51 wavelengths long, and with transducers having 7 fingers each. The measurements indicated a loaded  $Q$  of 1370 with the 50-ohm terminations used, and an unloaded  $Q$  of 2510. The solid lines show a theoretical computed response obtained using a transmission-line equivalent circuit for the resonators which is able to represent the resonators in both the pass and stop bands of the arrays.<sup>4</sup> The agreement appears good except for some error in the position of the stop-band-center of the arrays.

#### Filters Using Two-Port Resonators

Multiple resonator filters can be fabricated using cascaded two-port resonators of the form in Figs. 1(b) or 3(a). Such a filter is shown in Fig. 5 where a number of two-port, surface-wave resonators are indicated to be fabricated all on the same substrate with electrical connections between resonators. The coupling between resonators can be controlled by varying the number of fingers in the transducers or by adding decoupling capacitance.

The dashed lines and crosses in Fig. 6 show measured data for a filter using two resonators of the type used for Fig. 4. The solid lines in Fig. 6 show the theoretical computed response for this design using the transmission line equivalent circuit model.<sup>4</sup> Note that again the agreement between theory and experiment is very good except for the error due to the difference between the resonant frequency of the resonators and the array stopband center.

#### Conclusions

Surface-wave resonators provide the possibility for obtaining extremely small, relatively high- $Q$  resonators for filters at frequencies up to the lower microwave range. Their application may be most attractive for the UHF region where compact, high- $Q$  resonators presently do not exist.

#### References

1. 1974 Ultrasonics Symposium Proceedings, IEEE, New York, Cat. No. 74 CHO 896-1SU. Contains five papers on surface-wave resonators by various authors. See pp. 245-267, and 282-285.
2. 1975 Ultrasonics Symposium Proceedings, IEEE, New York, Cat. No. 75 CHO 994-4SU. See pp. 241-244, 269-298, 303-310, 381-384, and 395-399.
3. G. L. Matthaei, B. P. O'Shaughnessy, and F. Barman, "Relations for Analysis and Design of Surface-Wave Resonators," to be published in the March 1976 IEEE Trans. on Sonics and Ultrasonics.
4. G. L. Matthaei, F. Barman, E. B. Savage, and B. P. O'Shaughnessy, pp. 284-289 of Ref. 2 above.
5. W. P. Mason, Ed., Physical Acoustics, Vol. I - Part A, Academic Press, New York, 1964, Chapter 5.
6. H. J. Blinchikoff, "Low-Transient Intermediate-Band Crystal Filters," IEEE Trans. CAS-22, pp. 509-515, June 1975.
7. F. Ishihara, Y. Koyamada, and S. Yoshikawa, pp. 381-384 of Ref. 2 above.
8. S. C.-C. Tseng, and G. W. Lynch, pp. 282-285 of Ref. 1 above.

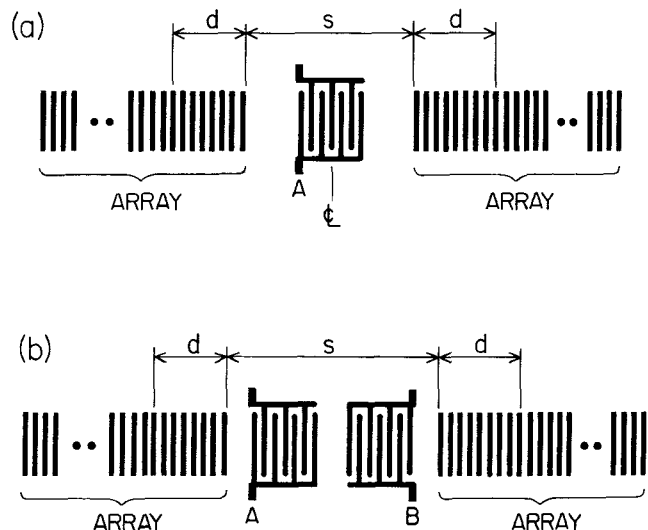


Fig. 1. (a) A one-port surface-wave resonator,  
(b) A two-port surface-wave resonator.

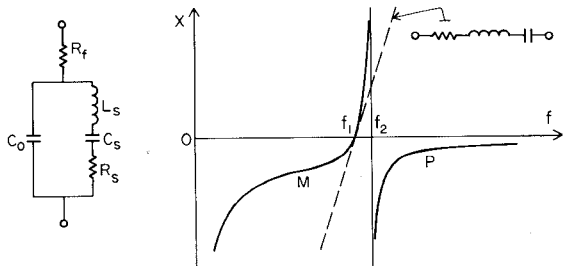


Fig. 2. Simplified circuits for surface-wave and conventional resonators, and their reactance characteristics.

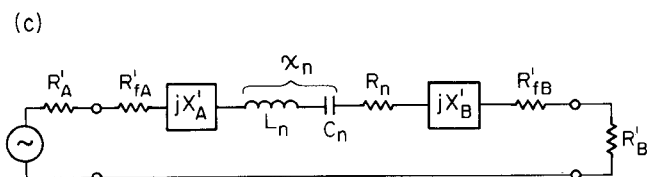
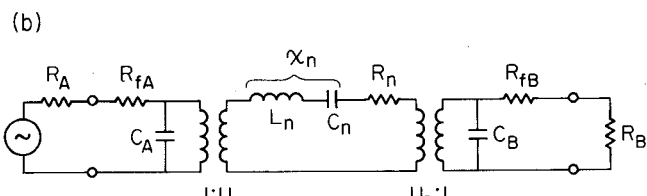
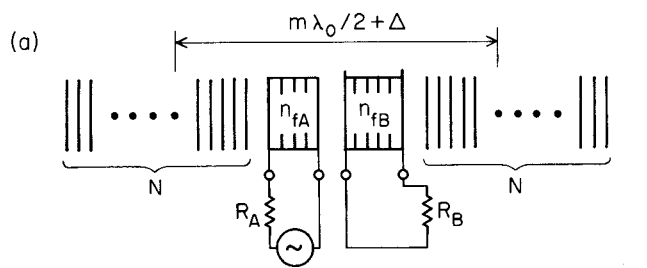


Fig. 3. (a) A two-port surface-wave resonator circuit.  
(b), (c) Equivalent circuits which apply for frequencies within the stop band of the arrays.

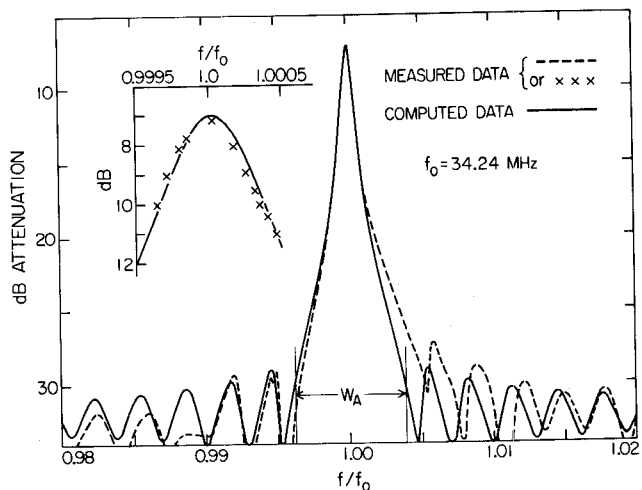


Fig. 4. Measured and computed characteristics for a trial two-port surface-wave resonator.

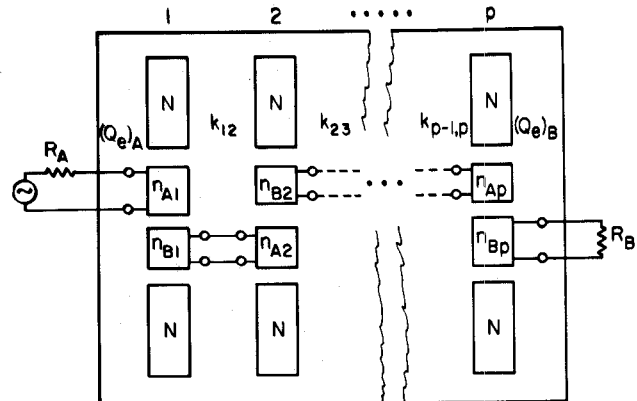


Fig. 5. A multiple-two-port-resonator surface-wave filter.

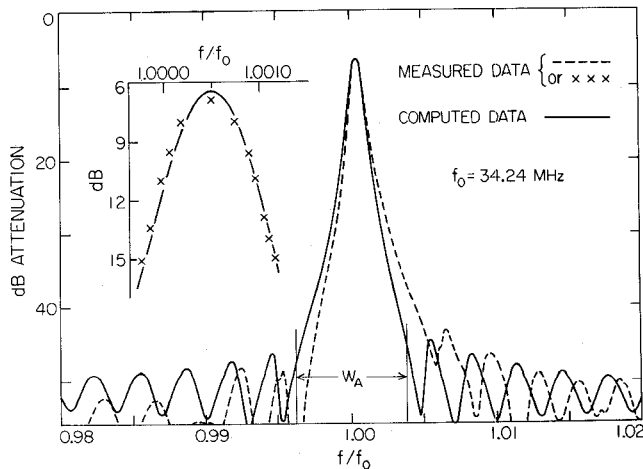


Fig. 6. Measured and computed responses for a two-resonator, surface-wave-resonator filter.